THz Spectroscopy by Frequency-Tuning Monochromatic THz Source: From Single Species to Gas Mixtures

Hongqian Sun, Yujie J. Ding, *Senior Member, IEEE*, and Ioulia B. Zotova

***Abstract*—Different gases have been successfully fingerprinted on the basis of the distinct transition frequencies measured by frequency tuning a THz source developed by us. Our further analysis illustrates that one can reliably separate isotopologues by measuring and comparing their rotational constants. Based on our investigation of the N_2O isotopologues, 29 rotational transition peaks were identified for the first time. For the gas mixtures, preliminary results indicate that one can identify the components of chemical species and the corresponding concentrations. Based on our spectroscopic results, the tunable THz source may offer a viable approach in the identifications and detections of chemical species.**

***Index Terms*—Identifications and detections of chemical species, rotational transitions, terahertz (THz), transmission and absorption spectroscopy.**

I. Introduction

RECENTLY,there have been consistent efforts dedicated to the spectroscopy and sensing applications in the THz spectral region (i.e., the frequency interval between 10^{11} Hz and 10^{13} Hz). Indeed, some researchers obtained the unique THz spectra for sucrose crystals, biomolecules, flames, explosives, water vapor, and various gases [1]–[10]. As reviewed in [11], the time-resolved THz spectroscopy has widely been used to investigate carrier dynamics. More importantly, since most of the chemical species in the vapor phase possess rather sharp and distinct absorption peaks, it is quite feasible to utilize THz spectroscopy for the chemical identification and detection. Generally, the absorption peaks in the THz range originate from the molecular rotational transitions. They are fundamentally different from those in the other spectral ranges, such as near IR. Based on the rotational transitions, some characteristic parameters, such as rotational constants, can be deduced in order to label and to identify the corresponding molecules. Therefore, in principle THz spectroscopy can be an effective method for fingerprinting and identifying chemical species in the vapor phase.

Currently, most of the applications of THz waves in spectroscopy are primarily hampered by the lack of suitable tunable THz sources and detectors. Although the THz time-domain spectroscopy and the Fourier transform IR spectroscopy have been utilized to reconstruct THz spectra for various materials, the spectral resolution is still limited [12]. To achieve higher spectral resolutions, backward-wave oscillator (BWO) tubes and photo mixing between two CO_2 lasers (TuFir) have been utilized by some spectroscopists in the past few years [12]–[14]. However, BWO tubes usually suffer from their short lifetimes (1000 h). In addition, each tube can only cover a relatively narrow frequency range (e.g., 200–300 GHz). On the other hand, since a photo mixer is mechanically fragile, it can be easily damaged by low electrical current or mechanical disturbances. Recently, there have been considerable efforts being devoted to the development of narrowband THz sources based on parametric processes [15]–[18], which appear to be quite promising for realizing one of the key applications in identifications and detections of chemical species.

In this paper, we report our results following the investigation of the molecular spectroscopy of the polar molecules from single species to mixtures of gases by frequency tuning a THz source developed by us [15]. Our results illustrate that such a source holds a promise for the applications of THz waves in identifications and detections of chemical species. The primary objective of this article is to report the spectroscopic results obtained by using such a source. This paper is organized as follows. In Section II, we provide the details of our experiments on the molecular spectroscopic study. All of the spectra measured by us and discussions of our results are summarized and presented in Section III. We will draw conclusions in Section IV.

II. Experimental Details

In our spectroscopic studies of polar molecules, we used a THz source implemented by frequency-mixing two near-IR laser beams [i.e., difference-frequency generation (DFG)] in a GaSe crystal [15]. According to the setup illustrated in Fig. 1, the first mixing beam was an output of a Nd:YAG laser at the wavelength of 1.064 μm (pulse duration, 10 ns; repetition rate, 10 Hz; pulse-to-pulse stability, $\pm 2\%$), and the second beam was the idler output from master oscillator/power oscillator (MOPO) emitting a wavelength tunable within 0.735–1.8 μm (pulse duration, 5 ns; repetition rate, 10 Hz; pulse-to-pulse stability, $\pm 8\%$). To prevent the GaSe crystal from optical damage, pulse energies of the two beams were attenuated to 6 and 3–7 mJ, respectively. After the GaSe crystal, the peak power of the THz source can reach 389 W at 203 μm (pulse duration, 5 ns; pulse energy, 2 μJ; pulse-to-pulse stability, $\pm 10\%$), whereas the output wavelength can be continuously

Manuscript received February 26, 2009; accepted March 03, 2009. Current version published February 24, 2010. This work was supported by the U.S. Army Research Office. The associate editor coordinating the review of this paper and approving it for publication was Dr. James Jensen.

H. Sun and Y. J. Ding are with the Department of Electrical and Computer Engineering, Center for Optical Technologies, Lehigh University, Bethlehem, PA 18015 USA (e-mail: hos4@lehigh.edu; yud2@lehigh.edu).

I. B. Zotova is with ArkLight, Center Valley, PA 18034 USA (e-mail: yzotova@hotmail.com).

Color versions of one or more of the figures in this paper are available online at http://ieeexplore.ieee.org.

Digital Object Identifier 10.1109/JSEN.2009.2038568

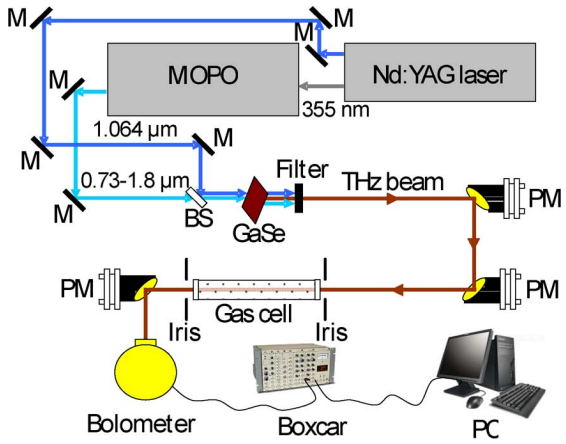

Fig. 1. Setup for measuring transmission spectrum: M, mirror; BS, beam splitter; PM, parabolic mirror. Although a bolometer was used, transmittances can be measured by using a pyroelectric detector operating at room temperature.

tuned between 58.2μm (172 cm^{-1}) and 3540 μm (2.82 cm^{-1}), with a typical linewidth of 0.36 cm^{-1} (11 GHz) [19]. In order to tune the output frequency of the THz source, one just needs to slightly tune the frequency of the MOPO output beam. Compared to the BWO tubes, this tunable THz source has a much longer lifetime and relies on a much simpler setup. Unlike the TuFir system, there are no fragile components, and therefore, such a THz source is much more robust. Using our THz source, the spectra can be conveniently measured based on the frequency-tuning scheme.

During our measurements, all of the chemical species were sealed in the single-pass gas cells. The side wall of each cell and the windows are made of quartz and either UV fused silica (^{12}CO and ^{13}CO) or fused quartz (for the rest), respectively. For the two CO isotopologues, the windows being wedged at 2° are mounted with a tilt angle of 11° ± 1° to eliminate the interference caused by the multiple reflections from the windows. For the rest of the chemical species, a vacuum reference cell was used to remove both the interference effect and the additional absorption caused by the windows. As a result, flat windows were used. The length of the gas cells was either 150 mm for CO isotopologues, HBr, NO, NH_3, and H_2S, or 200 mm for N_2O isotopologues, ^{12}CO/^{13}CO mixture, and HBr/HCl mixture.

As illustrated in Fig. 1, the THz signal was measured by a bolometer with its electrical output being measured by a boxcar integrator. Although we chose the bolometer, the signal levels for all of our measurements are much higher than the noise equivalent energy for the deuterated L-alanine doped triglycene sulphate pyroelectric energy meter operating at room temperature. All the measurements were made on the gas cells at room temperature. The output wavelength of the THz source was calibrated by comparing the frequencies of the observed water-vapor absorption peaks with those available from the high-resolution transmission molecular absorption (HITRAN) database [20]. For some of the gases investigated by us, i.e., HBr, N_2O isotopologues, NH_3, CO isotopologues mixture, and HBr/HCl mixture, the boxcar integrator was set to record 300 pulses in order to increase the SNR. Therefore, the THz signal measurement at each wavelength took about 1 min and the duration of time required to record each spectrum is about 300–400 min (i.e., those spectra in Figs. 8, 10, 12, 14, and 15). On the other hand, for the rest of the gases, 90 pulses were recorded. As a result, the spectra can be measured with a duration time of being more than three times shorter. These durations can be dramatically reduced if GaP is used as a DFG crystal [21].

III. Results and Discussions

A. Single Species

In this section, using the tunable THz source, we have measured the distinct rotational constants for CO isotopologues, the splitting of the ground energy level due to spin-orbital coupling for NO, 29 newly identified transitions for N_2O isotopologues, and inversion and inversion-rotational transitions for NH_3.

1) Carbon Monoxide (^{12}CO and ^{13}CO): Being the polar diatomic molecule exhibiting the simplest signature in the THz spectrum, it is natural for us to evaluate the performance of our THz spectrometer on CO. Generally, the rotational transition frequencies for diatomic and linear molecules can be predicted by

$$\nu = 2B(J+1) - 4D(J+1)^3 \approx 2B(J+1) \qquad (1)$$

where $B = h/8\pi^2 cI$ is rotational constant with I being the rotational moment of inertia and D is centrifugal distortion constant. Since B is usually much larger than D, one can consider the transition frequencies to be more or less linearly proportional to the rotational quantum number (J). Therefore, in the frequency domain the rotational transitions for CO are evenly spaced and exhibit a clear "comb" pattern.

There are several isotopologues of CO, among which ^{12}CO and ^{13}CO are ranked as the top two based on their natural abundances. Since different isotopologues have exactly the same chemical composition, accurate differentiation among them has been quite challenging to researchers. As demonstrated shortly, THz spectroscopy can be used to clearly identify them based on the different frequency spacings observed [i.e., $\Delta\nu = 2B$, see (1)]. This is due to the fact that different isotopologues have slightly different rotational moments of inertia and corresponding rotational constants.

During our experiment, we measured transmission spectra for both ^{12}CO (600 Torr) and ^{13}CO (600 Torr) at two different step sizes for the wavelength. First, we used a coarse one in order to determine the rough locations for all the transition peaks within a relatively broad range. As illustrated by Fig. 2, four pairs of rotational transitions were observable. We then switched to a fine one to just cover each transition peak. In Fig. 3, the same pairs of transitions were clearly resolved and the measured frequencies were tabulated in Table I. Although the lineshape of each transition peak should be fitted by using the van Vleck–Weisskopf model [22], the Lorentzian lineshape is sufficient to determine the peak frequency. Due to the relatively high pressure of CO, the linewidth broadening of 0.8 cm^{-1} is primarily caused by collisions between molecules, which is clearly resolvable by our tunable THz source.

As shown in Fig. 2, transmittance for both ^{12}CO and ^{13}CO decreases as frequency is increased. Such a monotonic decrease

TABLE I
PURE ROTATIONAL TRANSITION FREQUENCIES OF ^{12}CO AND ^{13}CO DEDUCED FROM FIGS. 3 AND 4

Transition	^{12}CO Theory (cm^{-1})	^{12}CO Measured (cm^{-1})	Deviation (cm^{-1})	^{13}CO Theory (cm^{-1})	^{13}CO Measured (cm^{-1})	Deviation (cm^{-1})
7←6	26.9	27.1	0.2	25.7	25.7	0
11←10	42.3	42.2	-0.1	40.4	40.4	0
12←11	46.1	46.1	0	44.1	44.1	0
13←12	49.9	50.0	0.1	47.7	47.8	0.1
14←13	53.8	53.8	0	51.4	51.4	0

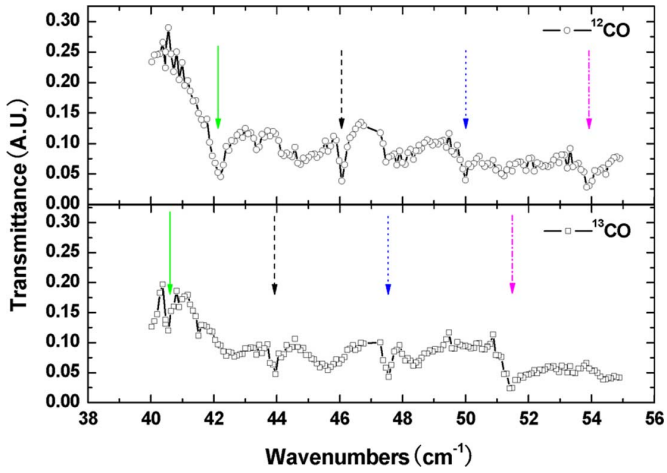

Fig. 2. Transmission spectra of ^{12}CO and ^{13}CO, measured by frequency tuning a THz source with a coarse tuning step size.

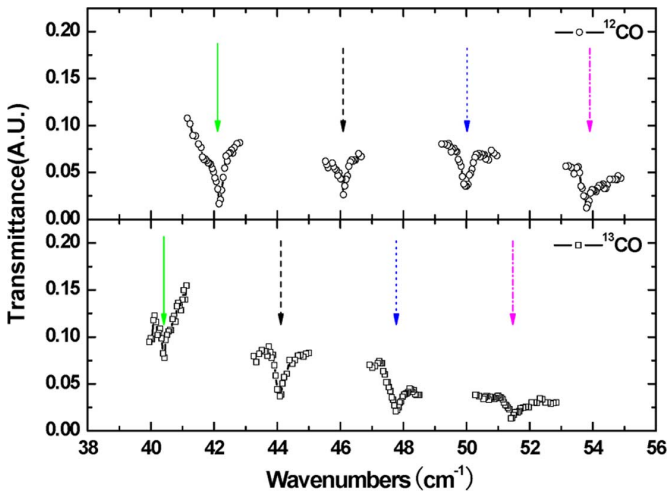

Fig. 3. Transmission spectra of ^{12}CO and ^{13}CO, measured by frequency tuning a THz source with a fine step size.

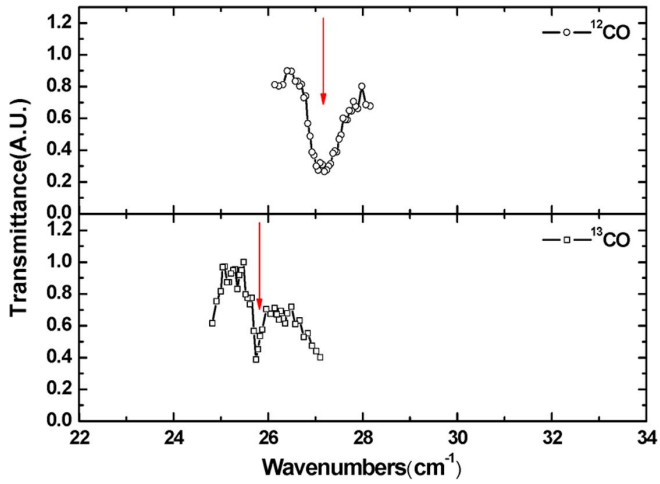

Fig. 4. Transmission spectra for $J = 7 \leftarrow 6$ transitions of ^{12}CO and ^{13}CO, measured by frequency tuning a THz source.

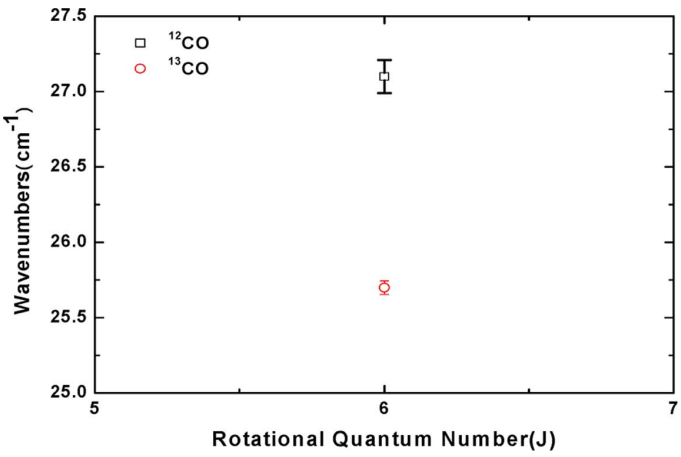

Fig. 5. $J = 7 \leftarrow 6$ rotational transitions of ^{12}CO (open squares) and ^{13}CO (open circles). Error bars designate the measurement errors.

is caused by the absorption from the two windows made of UV fused silica. Since our measurements were made in the air, some strong absorption peaks of water vapor may overlap and mask the absorption peaks of the CO molecules. Consequently, it is not possible for us to resolve the transition peaks for the CO molecules between 28 and 40 cm^{-1}. As the frequency of the THz source was tuned away from the H_2O absorption peaks, another pair of transitions $(J = 7 \leftarrow 6)$ were observed for the two CO isotopologues, see Fig. 4.

Overall, we have clearly resolved five pairs of transitions with their frequencies being tabulated in Table I, where the theoretical values are taken from the HITRAN database [20]. It is found that the largest deviation for the transition frequency is 0.2 cm^{-1}. The linewidth of our THz source and the MOPO wavelength deviation (i.e., on the order of 0.1 cm^{-1}) are the two major reasons for causing such measurement deviations. According to our error analysis, the measured transition frequencies have relatively good accuracies, see Fig. 5. As shown in Fig. 6, by linearly fitting the data for rotational transition frequency versus rotational quantum number, we have obtained the rotational constants to be 1.91 ± 0.01 and 1.84 ± 0.00 cm^{-1} for ^{12}CO and ^{13}CO, respectively. These values are in good agreements with the

TABLE II
PURE ROTATIONAL TRANSITION FREQUENCIES OF HBR, DEDUCED FROM FIG. 7

Transition	Theory (cm^{-1})	Measured (cm^{-1})	Deviation (cm^{-1})	K_p ($cm^{-1}Torr^{-1}$)
1←0	16.7	16.7	0	1.04×10^{-4} $\pm0.07\times10^{-4}$
2←1	33.4	33.4	0	6.92×10^{-4} $\pm0.21\times10^{-4}$
3←2	50.1	50.2	0.1	N.A.

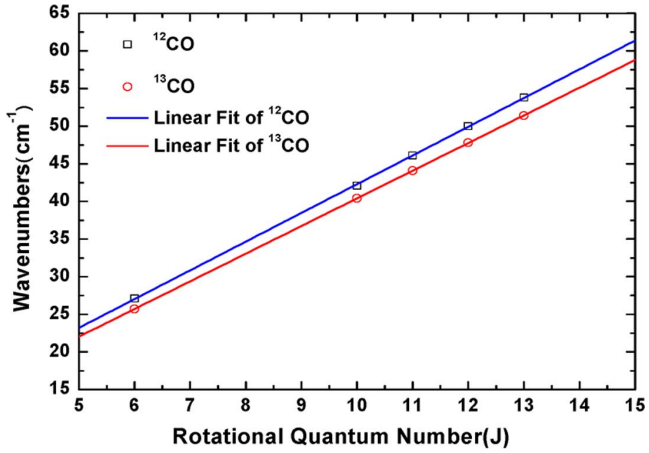

Fig. 6. Transition frequency was measured versus rotational quantum number for ^{12}CO (open squares) and ^{13}CO (open circles). Solid curves correspond to linear least-square fitting to data.

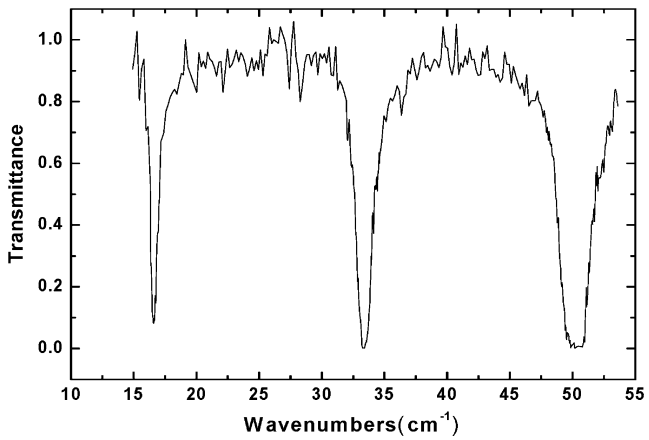

Fig. 7. Transmission spectrum of HBr, measured by using our THz source.

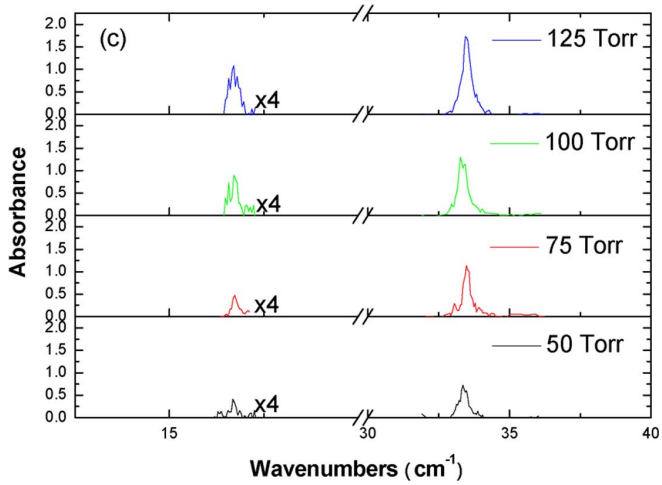

Fig. 8. Absorbance of HBr versus frequency at different pressures for two rotational transitions (i.e., $J = 1 \leftarrow 0$ and $J = 2 \leftarrow 1$). To make the $J = 1 \leftarrow 0$ transition more visible, the absorbance is multiplied by 4.

reported values (i.e., $1.9211989340 \pm 0.0000000001$ cm^{-1}, $1.83670043 \pm 0.00000001$ cm^{-1}) [13], [14]. Since the difference between the rotational constants, 0.07 cm^{-1}, is large enough, we have demonstrated that THz spectroscopy is a reliable technique for identifying the two CO isotopic variants.

2) Hydrogen Bromide (HBr): As reported previously, this chemical species being present in the stratosphere can be used as an indicator for ozone depletion [23].

As shown in Fig. 7, within the range of 15–55 cm^{-1}, we identified three absorption peaks originating from rotational transitions for HBr under 600 Torr. All of the three transition frequencies measured by us, and the corresponding measurement errors have been tabulated in Table II. Compared with CO, the frequency spacing between the transition peaks for HBr is much larger. This is due to the fact that HBr has a much smaller rotational moment of inertia. By linearly fitting the data, the rotational constant for HBr is determined to be 8.38 ± 0.01 cm^{-1}, which is about 4.5 times larger than those for the CO isotopologues. In addition, the measured rotational constant is also quite consistent with the previously reported value (8.3428 cm^{-1} in [24]). One can see from Fig. 7 that by measuring the THz beam propagating through a vacuum cell as background signal, we have removed the monotonically decreased absorption slope caused by the two windows. As a result, the vertical axis for Fig. 7 is the actual transmittance for HBr.

According to Beer's Law, an absorption coefficient for HBr κ_p can be directly deduced from the minimum transmittance for each transition peak by using the following expression:

$$\kappa_p = -\frac{\ln(T)}{Pl} \tag{2}$$

where T is the transmittance, P is the pressure of HBr, and l is the length of the HBr gas cell. Based on our measurements made on a set of four HBr cells under different pressures (i.e., $P \approx 50$, 75, 100, and 125 Torr, and $l \approx 20$ cm), see Fig. 8, we have determined the absorption coefficients for $J = 1 \leftarrow 0$ and $J = 2 \leftarrow 1$ to be $1.04 \times 10^{-4} \pm 0.07 \times 10^{-4}$ and $6.92 \times 10^{-4} \pm 0.21 \times 10^{-4}$ cm^{-1} Torr^{-1}, respectively, see Table II. Unfortunately, due to the saturation of the absorption for $J = 3 \leftarrow 2$, the corresponding absorption coefficient cannot be obtained from our measurements. In Section III-B2, we illustrate how to determine the partial pressure for HBr in a mixture using these absorption coefficients.

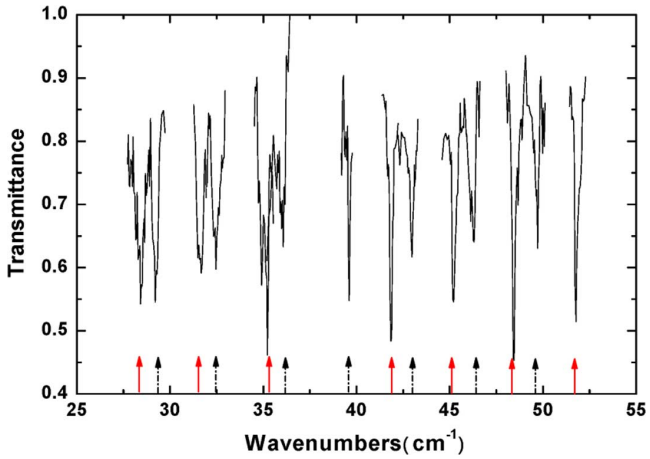

Fig. 9. Transmission spectrum of NO, measured by using our frequency-tunable THz source. Red solid arrows and black dashed arrows mark rotational transitions from two ground energy states, $^2\Pi_{1/2}$ and $^2\Pi_{3/2}$, respectively.

3) Nitric Oxide (NO): NO is known as an important signaling molecule within the bodies of mammals. On the other hand, it is also a toxic air pollutant produced by automobile engines and power plants. Since it is a free radical, it can react with oxygen to form NO_2. More importantly, it was found this molecule is responsible for initiating the catalytic ozone loss cycle in the stratosphere [25].

Unlike other diatomic molecules, NO is the only stable radical with one unpaired electron. Due to the spin-orbital coupling of this electron, the ground state of NO is split into two energy levels labeled by $^2\Pi_{1/2}$ and $^2\Pi_{3/2}$ [26]. Since the frequency difference between these two states is 122 cm^{-1}, which is relatively small, there are a large number of the NO molecules being thermally excited to the higher lying state $(^2\Pi_{3/2})$. Therefore, the THz spectrum of NO consists of two sets of the rotational transitions corresponding to the two split ground states. Since the two sets of rotational transitions have slightly different frequency spacings, different effective rotational constants should be derived for each split state, i.e., $B(^2\Pi_{1/2})$ and $B(^2\Pi_{3/2})$.

To investigate rotational transitions, we filled a quartz gas cell with NO at 200 Torr. As shown in Fig. 9, one can clearly observe several paired transition peaks. Due to the Boltzmann distribution, a higher fraction of the NO molecules stays at $^2\Pi_{1/2}$. Therefore, the absorption for the rotational transitions starting from $^2\Pi_{1/2}$ is always larger than that from $^2\Pi_{3/2}$. Within 28–55 cm^{-1}, one can also identify two unpaired transitions. This is due to the fact that the other two transition peaks of NO significantly overlap with the absorption peaks of the water vapor. By linearly fitting the transition frequencies measured by us, see Tables III and IV, the rotational constants for the two split energy states are determined to be $B(^2\Pi_{1/2}) = 1.67\pm 0.01^{-1}$ cm and $B(^2\Pi_{3/2}) = 1.72\pm 0.01^{-1}$ cm , which are quite close to 1.671854 ± 0.000081 and 1.720178 ± 0.000062 cm^{-1} [26]. Based on these rotational constants, the unperturbed rotational constant can be calculated by taking an average over the two as 1.70 ± 0.01 cm^{-1}. This value is rather consistent with 1.696008 ± 0.000072 cm^{-1} [26].

TABLE III
PURE ROTATIONAL TRANSITION FREQUENCIES OF NO FROM $^2\Pi_{1/2}$

Transition	Measured (cm^{-1})	Deviation (cm^{-1})
8.5←7.5	28.4	0.0
9.5←8.5	31.7	-0.1
10.5←9.5	35.2	0.1
12.5←11.5	41.8	0.0
13.5←12.5	45.2	0.1
14.5←13.5	48.4	-0.1
15.5←14.5	51.7	-0.1

TABLE IV
PURE ROTATIONAL TRANSITION FREQUENCIES OF NO FROM $^2\Pi_{3/2}$

Transition	Measured (cm^{-1})	Deviation (cm^{-1})
8.5←7.5	29.2	0.0
9.5←8.5	32.5	-0.1
10.5←9.5	36.0	-0.1
11.5←10.5	39.6	0.1
12.5←11.5	42.9	0.0
13.5←12.5	46.3	0.0
14.5←13.5	49.7	-0.1

Compared to the other diatomic molecules, such as CO and HBr, the double sets of evenly spaced rotational transitions are unique enough such that one can use them to identify NO.

4) Isotopologues of Nitrous Oxide ($^{14}N^{14}NO$, $^{14}N^{15}NO$, and $^{15}N^{14}NO$): N_2O is commonly known as "laughing gas." It has been used in surgery and dentistry for its anaesthetic and analgesic effects. Although N_2O is a minor constituent of the atmosphere, it is one of the major green house gases, which play an important role in global warming [27]. N_2O also reacts with ozone in the stratosphere, causing the ozone depletion [28]. Due to its linear molecular structure, the "comb" pattern in the THz spectrum can be used as a frequency standard.

Similar to CO, N_2O naturally consists of several isotopologues. In the past, most of the previous rotational transition measurements were performed on the dominant isotopologue, i.e., $^{14}N^{14}NO$ [29]. For $^{14}N^{15}NO$ and $^{15}N^{14}NO$, however, very few reports can be found [29], [30]. By frequency tuning our THz source, we have identified 29 new transition peaks for these two isotopic variants. The rotational constants for the three isotopologues, determined by us, are different from one another.

The gas cells were filled with the three isotopic variants at either 200 ($^{14}N^{14}NO$) or 400 Torr ($^{14}N^{15}NO$, $^{15}N^{14}NO$). As illustrated by Fig. 10, within 15–37.4 cm^{-1}, we have identified 16, 26, and 26 transition peaks for $^{14}N^{14}NO$, $^{14}N^{15}NO$, and $^{15}N^{14}NO$, respectively. For $^{14}N^{14}NO$, all of the 16 transition peaks were measured previously [29]. As one can see from Table V, these 16 transitions are in good agreements with the theoretical values [20]. On the other hand, for $^{14}N^{15}NO$ and $^{15}N^{14}NO$, we have identified 14 and 15 new transition peaks. By using (1) to fit the transition frequencies determined from Fig. 10, see Table V, we have obtained $B \approx 0.416 \pm 0.001$, $B \approx 0.420\pm0.001$, and $B \approx 0.403\pm0.001$ cm^{-1} for $^{14}N^{14}NO$, $^{14}N^{15}NO$, and $^{15}N^{14}NO$, respectively. Based on different rotational constant values, one can reliably differentiate between $^{14}N^{14}NO$ and $^{15}N^{14}NO$ or $^{14}N^{15}NO$ and $^{15}N^{14}NO$. However,

TABLE V
PURE ROTATIONAL TRANSITION FREQUENCIES OF $^{14}N^{14}NO$, $^{14}N^{15}NO$, AND $^{15}N^{14}NO$, DEDUCED FROM FIGS. 10

Transition	$^{14}N^{14}NO$ (cm^{-1})	Deviation (cm^{-1})	$^{14}N^{15}NO$ (cm^{-1})	Deviation (cm^{-1})	$^{15}N^{14}NO$ (cm^{-1})	Deviation (cm^{-1})
19←18			15.9	0.0	15.4	0.0
20←19			16.8	0.0	16.3	0.1
21←20			17.6	0.0	17.1	0.1
22←21			18.3	-0.1	17.8	0.0
23←22			19.3	0.0	18.6	0.0
24←23			20.1	0.0	19.5	0.1
25←24			20.9	0.0	20.2	0.0
26←25			21.7	-0.1	21.1	0.1
27←26			22.6	0.0	21.9	0.1
28←27	23.4	0.0	23.4	0.0	22.7	0.0
29←28	24.2	-0.1	24.3	0.0	23.5	0.0
30←29	25.2	0.1	25.1	0.0	24.3	0.0
31←30	25.9	-0.1	25.9	-0.1	25.1	0.0
32←31	26.8	0.0	26.8	0.0	25.9	0.0
33←32	27.7	0.1	27.6	0.0	26.7	0.0
34←33	28.5	0.0	28.5	0.0	27.6	0.1
35←34	29.3	0.0	29.3	0.0	28.3	0.0
36←35	30.1	0.0	30.2	0.1	29.1	0.0
37←36	30.9	-0.1	30.9	-0.1	29.9	0.0
38←37	31.8	0.0	31.8	0.0	30.9	0.2
39←38	32.6	0.0	32.7	0.1	31.7	0.2
40←39	33.5	0.0	33.4	-0.1	32.4	0.1
41←40	34.3	0.0	34.4	0.1	33.1	-0.1
42←41	35.1	0.0	35.3	0.2	34.0	0.0
43←42	35.9	-0.1	36.1	0.1	34.7	-0.1
44←43			36.9	0.1	35.6	0.0

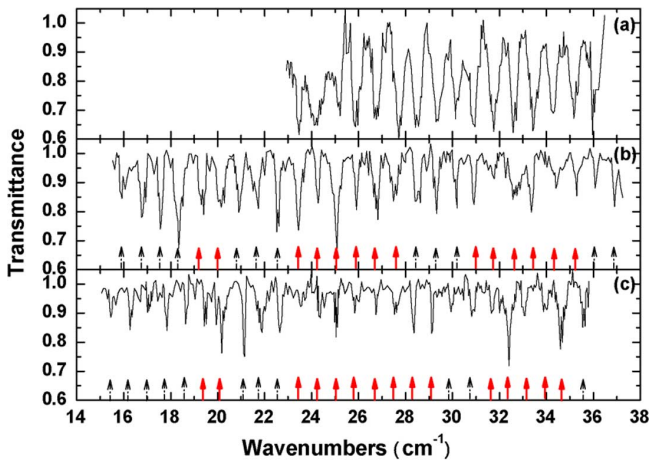

Fig. 10. Transmission spectra of N_2O, measured by using our frequency-tunable THz source: (a) $^{14}N^{14}NO$; (b) $^{14}N^{15}NO$; and (c) $^{15}N^{14}NO$. Red solid arrows mark newly identified rotational transitions; black dashed arrows mark previously identified rotational transitions.

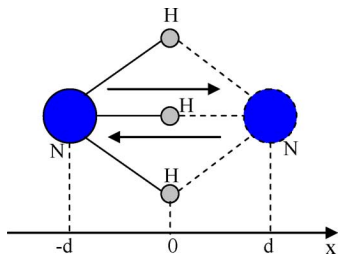

Fig. 11. Inversion transition for an N atom within each NH_3 molecule.

in order to differentiate between $^{14}N^{14}NO$ and $^{14}N^{15}NO$, the linewidth of our THz source must be further reduced.

Compared with CO, the rotational constants for N_2O are much lower. This is due to the fact that N_2O has much larger reduced masses. According to (1), this results in a much lower rotational constants. Therefore, the frequency spacings for N_2O are much narrower than those for CO.

5) Ammonia (NH_3): NH_3 is perhaps one of the simplest molecules undergoing inversions. However, most of the previous results on this molecule and its epoch-making applications, such as the first maser and the NH_3 molecular clock, were all related to the inversion transitions occurring within the ground vibrational state ($\nu_2 = 0$) in the microwave range. Since the inversion and inversion-rotational transitions within the excited vibrational states (i.e., $\nu_2 \geq 1$) have higher frequencies, the investigation of these transitions has been severely hampered by the lack of a THz source emitting sufficiently high output powers within a broadly tunable frequency range. So far, limited results have been reported by using BWO tubes [31] and a photo mixer based on a low-temperature-grown GaAs crystal [32].

In this section, we present our results of the transmission spectrum on NH_3. We are focusing on the inversion and inversion-rotational transitions within $\nu_2 = 1$ excited state. One can see from Fig. 11 that a nitrogen atom can tunnel through the plane formed by three hydrogen atoms within each NH_3 molecule. As a result, NH_3 forms double-well vibrational potential energy states. Consequently, each rotational energy state is split into a doublet labeled by s and a, corresponding to the symmetric and antisymmetric states, respectively. According to the selection rule for transitions, the inversion transitions and inversion-rotational transitions take place as follows: $J_a \leftarrow J_s, (J+1)_a \leftarrow J_s$, and $(J+1)_s \leftarrow J_a$.

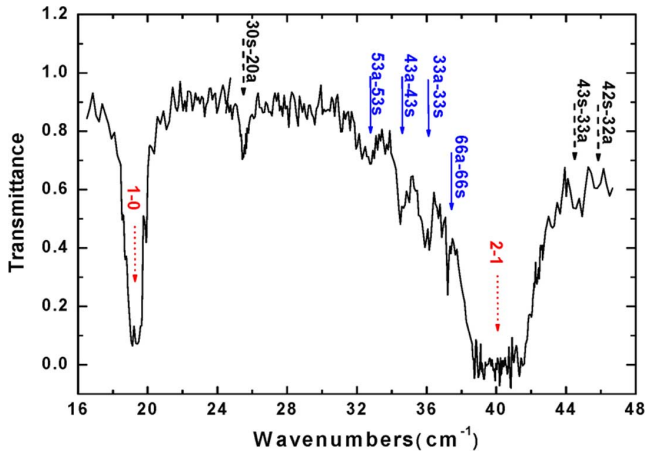

Fig. 12. Transmission spectrum measured on NH_3 by frequency tuning our THz source. Blue solid arrows mark inversion transitions; black dashed arrows mark inversion-rotational transitions, both within $v_2 = 1$. Red dotted arrows mark rotational transitions within $v_2 = 0$.

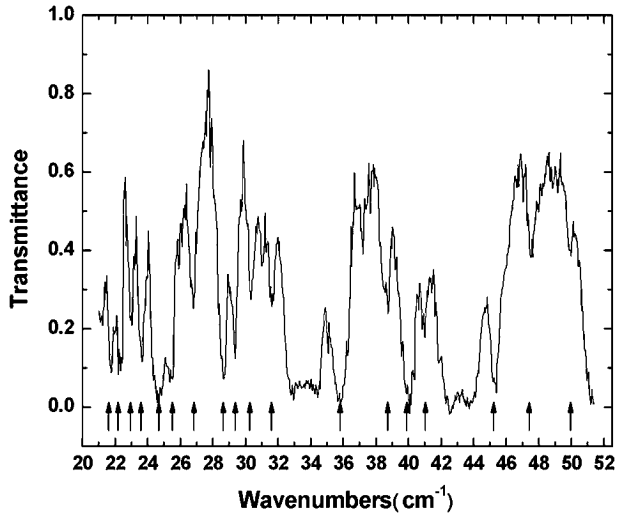

Fig. 13. Transmission spectrum measured on H_2S, using our frequency-tunable THz source.

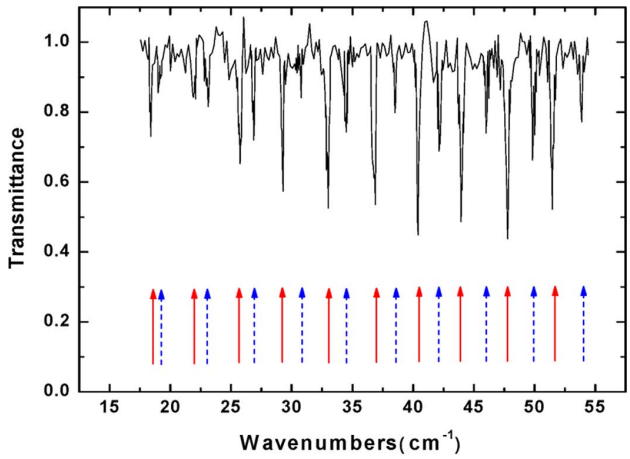

Fig. 14. Transmission spectrum measured on a mixture of ^{12}CO and ^{13}CO. Blue dashed arrows mark transitions for ^{12}CO; red solid arrows mark transitions for ^{13}CO.

Since the absorption due to the transitions within $\nu_2 = 1$ is extremely weak, we set the pressure of the NH_3 cell to 600 Torr. As one can see from Fig. 12, seven peaks have been clearly identified. Among them, the four peaks at 32.7, 34.5, 36.0, and 37.2 cm^{-1} correspond to the inversion transitions, whereas the rest at 25.6, 44.7, and 45.8 cm^{-1} originate from the inversion-rotational transitions, all within $\nu_2 = 1$. Besides these seven transition peaks, we also identified two dominant peaks at 19.2 and 40.0 cm^{-1}, respectively, see Fig. 12. They originate from the rotational transitions within $\nu_2 = 0$ (ground state). From the energy splitting between the antisymmetric and symmetric rotational states, periods required for the inversion to occur can be determined by

$$\tau = \frac{h}{2\Delta\varepsilon} \tag{3}$$

where h is the Planck constant. Using (3), we have estimated the periods for the inversions to be 510, 483, 463, and 448 fs for $53a \leftrightarrow 53s, 43a \leftrightarrow 43s, 33a \leftrightarrow 33s$, and $66a \leftrightarrow 66s$, respectively. Therefore, these periods can be confirmed by using ultrafast THz pulses.

6) Hydrogen Sulfide (H_2S): As discussed earlier, both diatomic and linear molecules exhibit evenly spaced transition peaks in the THz frequency range. However, for asymmetric top molecules, such as H_2S, its rotational transitions typically spread over the entire THz frequency range without an obvious pattern [33], making it challenging to identify. H_2S, being a toxic and flammable gas, is usually produced by the bacterial breakdown of sulfates in the absence of oxygen.

By frequency tuning our THz source within 21–51.4 cm^{-1}, we measured the transmission spectrum of H_2S at 600 Torr, see Fig. 13. According to Table VI, the transition frequencies deduced from Fig. 13 are in good agreements with the theoretical values [20]. Indeed, the maximum deviation for the transition frequencies measured by us is 0.1 cm^{-1}. However, within 32.5–34.7 and 42.3–44.1 cm^{-1}, only two strong absorption peaks corresponding to $3_{03} \leftarrow 2_{12}$ and $4_{14} \leftarrow 3_{03}$ can be identified. Due to the pressure broadening, other weak absorption peaks within this range have been masked by these two dominant transitions.

7) Mixture of ^{12}CO and ^{13}CO: Consider a mixture of ^{12}CO and ^{13}CO. Both of them were filled into the cell at 300 Torr. As one can see from Fig. 14, all the transition peaks within 17.5–54.5 cm^{-1} were clearly identified. Apparently, under such a pressure there is no overlap among the transition peaks originating from ^{12}CO and ^{13}CO. One can also observe that the separation between the two paired transition peaks is increasing as the frequency is increased. This is caused by the increasing rotational quantum number J, see (1).

8) Mixture of HCl and HBr: Consider now the mixture of HBr and HCl. The transmission spectrum of the mixture was measured at 250 Torr for each of the two constituents. As shown in Fig. 15, one can clearly identify three and two transition peaks originating from HBr and HCl, respectively. Using (2) whereby κ_p is measured by us, see Table II, as shown earlier, we have estimated the partial pressures for HBr to be 241 and 235 Torr based on the transitions of $J = 1 \leftarrow 0$ and $J = 2 \leftarrow 1$,

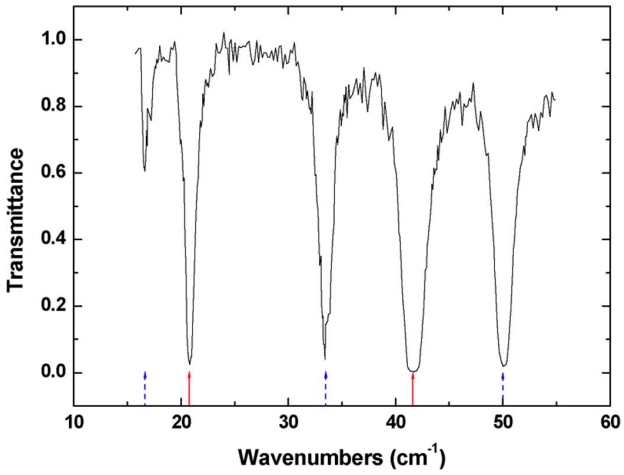

Fig. 15. Transmission spectrum measured for a mixture of HBr and HCl. Blue dashed arrows—HBr; red solid arrows—HCl.

TABLE VI
PURE ROTATIONAL TRANSITION FREQUENCIES OF H_2S, DEDUCED FROM FIG. 13

Transition	Theory (cm^{-1})	Measured (cm^{-1})	Deviation (cm^{-1})
$4_{41}\leftarrow4_{32}$	21.7	21.7	0.0
$4_{22}\leftarrow4_{13}$	22.2	22.3	0.1
$2_{02}\leftarrow1_{11}$	22.9	23.0	0.1
$3_{12}\leftarrow3_{03}$	23.6	23.7	0.1
$2_{12}\leftarrow1_{01}$	24.6	24.6	0.0
$4_{32}\leftarrow4_{23}$	25.5	25.5	0.0
$5_{42}\leftarrow5_{33}$	26.7	26.7	0.0
$6_{52}\leftarrow6_{43}$	28.5	28.6	0.1
$7_{43}\leftarrow7_{34}$	29.4	29.3	-0.1
$7_{70}\leftarrow7_{61}$	30.4	30.4	0.0
$6_{33}\leftarrow6_{24}$	31.6	31.7	0.1
$2_{21}\leftarrow1_{10}$	35.8	35.8	0.0
$9_{54}\leftarrow9_{45}$	38.5	38.6	0.1
$3_{12}\leftarrow2_{21}$	39.9	40.0	0.1
$8_{44}\leftarrow8_{35}$	40.9	41.0	0.1
$3_{22}\leftarrow2_{11}$	45.3	45.3	0.0
$11_{65}\leftarrow11_{56}$	47.4	47.5	0.1
$10_{55}\leftarrow10_{46}$	49.8	49.9	0.1

respectively. Therefore, the partial pressure for HBr is estimated to be 238 Torr after taking an average.

IV. CONCLUSION

By frequency tuning our THz source, we have measured transmission spectra for a class of chemical species and a couple of the mixtures of isotopic variants and gases. For all the diatomic molecules studied by us, transition peaks are evenly spaced in terms of their frequencies. For the mixtures of the diatomic molecules, we have identified all the transition peaks originating from the two constituents. For the mixture of HBr and HCl, we have determined the partial pressure for HBr. For the triatomic molecules, such as $^{14}N^{14}NO$, $^{14}N^{15}NO$, and $^{15}N^{14}NO$, we have measured the transition peaks that can be used to fingerprint them. Furthermore, for $^{14}N^{15}NO$ and $^{15}N^{14}NO$, we identified 29 new transition peaks. For NH_3, we have observed the inversion transitions and inversion-rotational transitions within the first excited vibrational state and calculated periods for the inversions. Finally, for asymmetric top molecules, such as H_2S, transition peaks do not form an obvious pattern. Most of the transition frequencies measured by us are quite consistent with the previous theoretical values. We have indeed demonstrated that our widely tunable monochromatic THz source holds a promise for the identifications and detections of chemical species.

REFERENCES

[1] J. Kröll, J. Darmo, and K. Unterrainer, "Terahertz optical activity of sucrose single crystals," *Vib. Spectrosc.*, vol. 43, pp. 324–329, Mar. 2007.
[2] J. Kitagawa, T. Ohkubo, N. Onuma, and Y. Kadoya, "THz spectroscopic characterization of biomolecule/water systems by compact sensor chips," *Appl. Phys. Lett.*, vol. 89, pp. 41114-1–41114-3, Jul. 2006.
[3] A. Markelz, S. Whitmire, J. Hillebrecht, and R. Birge, "THz time domain spectroscopy of biomolecular conformational modes," *Phys. Med. Biol.*, vol. 47, pp. 3797–3805, Oct. 2002.
[4] R. A. Cheville and D. Grischkowsky, "Far-infrared terahertz time-domian spectroscopy of flames," *Opt. Lett.*, vol. 20, pp. 1646–1648, Mar. 1995.
[5] H. Liu, Y. Chen, G. J. Bastiaans, and X.-C. Zhang, "Detection and identification of explosive RDX by THz diffuse reflection spectroscopy," *Opt. Exp.*, vol. 14, pp. 415–423, Jan. 2006.
[6] D. J. Cook, B. K. Decker, G. Maislin, and M. G. Allen, "Through container THz sensing applications for explosives screening," in *Proc. SPIE*, 2004, vol. 5354, pp. 55–62.
[7] M. S. Brown, G. J. Fiechtner, J. V. Rudd, D. A. Zimdars, M. Warmuth, and J. R. Gord, "Water-vapor detection using asynchronous THz sampling," *Appl. Spectrosc.*, vol. 60, pp. 261–265, Mar. 2006.
[8] J. F. Federici, B. Schulkin, H. Feng, D. Gary, R. Barat, F. Oliveira, and D. Zimdars, "THz imaging and sensing for security applications-explosives, weapons and drugs," *Semicond. Sci. Technol.*, vol. 20, pp. s266–s280, Jun. 2005.
[9] F. C. De Lucia and D. T. Petkie, "THz gas sensing with submillimeter techniques," in *Proc. SPIE*, 2005, vol. 5790, pp. 44–53.
[10] G. A. Blake, K. B. Laughlin, R. C. Cohen, K. L. Busarow, D.-H. Gwo, C. A. Schmuttenmaer, D. W. Steyert, and R. J. Saykally, "Tunable far-infrared laser spectrometers," *Rev. Sci. Instrum.*, vol. 62, pp. 1693–1700, Jul. 1991.
[11] , D. Mittleman, Ed., *Sensing With Terahertz Radiation*. New York: Springer-Verlag, 2003.
[12] C. A. Schmuttenmaer, "Exploring dynamics in the far-infrared with terahertz spectroscopy," *Chem. Rev.*, vol. 104, pp. 1759–1779, Mar. 2004.
[13] G. Winnewisser, S. P. Belov, Th. Klaus, and R. Schieder, "Sub-Doppler measurements on the rotational transitions of carbon monoxide," *J. Mol. Spectrosc.*, vol. 184, pp. 468–472, Aug. 1997.
[14] L. R. Zink, P. De Natale, F. S. Pavone, M. Prevedelli, K. M. Evenson, and M. Inguscio, "Rotational far infrared spectrum of ^{13}CO," *J. Mol. Spectrosc.*, vol. 143, pp. 304–310, Oct. 1990.
[15] W. Shi and Y. J. Ding, "A monochromatic and high-power THz source tunable in the range of 2.7–38.4 μm and 58.2–3540 μm for variety of potential applications," *Appl. Phys. Lett.*, vol. 84, pp. 1635–1637, Mar. 2004.
[16] T. Taniuchi, S. Okada, and H. Nakanishi, "Widely-tunable THz-wave generation in 2–20 THz range from DAST crystal by nonlinear difference frequency mixing," *Electron. Lett.*, vol. 40, no. 1, pp. 60–62, Jan. 2004.
[17] T. J. Edwards, D. Walsh, M. B. Spurr, C. F. Rae, M. H. Dunn, and P. G. Browne, "Compact source of continuously and widely-tunable terahertz radiation," *Opt. Exp.*, vol. 14, pp. 1582–1589, Feb. 2006.
[18] S. Y. Tochitsky, C. Sung, S. E. Trubnick, C. Joshi, and K. L. Vodopyanov, "High-power tunable, 0.5–3 THz radiation source based on nonlinear difference frequency mixing of CO_2 laser lines," *J. Opt. Soc. Amer. B*, vol. 24, pp. 2509–2516, Aug. 2007.
[19] Y. J. Ding and W. Shi, "Observation of THz to near-infrared parametric conversion in $ZnGeP_2$ crystal," *Opt. Exp.*, vol. 14, no. 18, pp. 8311–8316, Sep. 2006.

[20] L. S. Rothman, D. Jacquemart, A. Barbe, D. C. Benner, M. Birk, L. R. Brown, M. R. Carleer, C. Chackerian Jr., K. Chance, L. H. Coudert, V. Dana, V. M. Devi, J.-M. Flaud, R. R. Gamache, A. Goldman, J.-M. Hartmann, K. W. Jucks, A. G. Maki, J.-Y. Mandin, S. T. Massie, J. Orphal, A. Perrin, C. P. Rinsland, M. A. H. Smith, J. Tennyson, R. N. Tolchenov, R. A. Toth, J. V. Auwera, P. Varanasi, and G. Wagner, "The HITRAN 2004 molecular spectroscopic database," *J. Quant. Spectrosc. Rad. Transf.*, vol. 96, pp. 139–204, Dec. 2005.

[21] W. Shi and Y. J. Ding, "Tunable terahertz waves generated by mixing two copropagating infrared beams in GaP," *Opt. Lett.*, vol. 30, pp. 1030–1032, May 1, 2005.

[22] H. Harde, R. A. Cheville, and D. Grischkowsky, "Terahertz studies of collision-broadened rotational lines," *J. Phys. Chem. A*, vol. 101, pp. 3646–3660, May 1997.

[23] B. J. Finlayson-Pitts, F. E. Livingston, and H. N. Berko, "Ozone destruction and bromine photochemistry at ground level in the arctic spring," *Nature*, vol. 343, pp. 622–625, Feb. 1990.

[24] G. Jones and W. Gordy, "Submillimeter-wave spectra of HCl and HBr," *Phys. Rev.*, vol. 136, pp. A1229–A1232, Nov. 1964.

[25] D. M. Leahey and M. C. Hansen, "Observational evidence of ozone depletion by nitric oxide at 40 km downwind of a medium size city," *Atmos. Environ.*, vol. 24, pp. 2533–2540, 1990.

[26] R. T. Hall and J. M. Dowling, "Pure rotational spectrum of nitric oxide," *J. Chem. Phys.*, vol. 45, pp. 1899–1903, Sep. 1966.

[27] D. A. Lashof and D. R. Ahuja, "Relative contributions of greenhouse gas emissions to global warming," *Nature*, vol. 344, pp. 529–531, Apr. 1990.

[28] World Meteorological Organization, Scientific assessment of ozone depletion: 2006 Geneva, Switzerland, WMO Global Ozone Research and Monitoring Project-Rep. 50, 2007.

[29] B. J. Drouin and F. W. Maiwald, "Extended THz measurements of nitrous oxide, N_2O," *J. Mol. Spectrosc.*, vol. 236, pp. 260–262, Apr. 2006.

[30] I. Morino, M. Fabian, H. Takeo, and K. M. T. Yamada, "High-J rotational transitions of NNO measured with the NAIR terahertz spectrometer," *J. Mol. Spectrosc.*, vol. 185, pp. 142–146, May 1997.

[31] S. P. Belov, L. I. Gershstein, A. F. Krupnov, A. V. Maslovski, Š. Urban, V. Špirko, and D. Papoušek, "Inversion and inversion-rotation spectrum of $^{14}NH_3$ in the ν_2 excited state," *J. Mol. Spectrosc.*, vol. 84, pp. 288–304, Nov. 1980.

[32] P. Chen, J. C. Pearson, H. M. Pickett, S. Matsuura, and G. A. Blake, "Measurements of $^{14}NH_3$ in the $\nu_2 = 1$ state by a solid-state, photomixing, THz spectrometer, and a simultaneous analysis of the microwave, terahertz, and infrared transitions between the ground and ν_2 inversion-rotation levels," *J. Mol. Spectrosc.*, vol. 236, pp. 116–126, Mar. 2006.

[33] S. P. Belov, K. M. T. Yamada, G. Winnewisser, L. Poteau, R. Bocquet, J. Demaison, O. Polyansky, and M. Y. Tretyakov, "Terahertz rotational spectrum of H_2S," *J. Mol. Spectrosc.*, vol. 173, pp. 380–390, Oct. 1995.

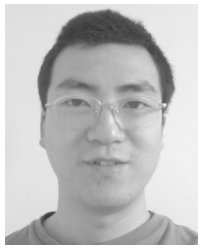

Hongqian Sun received the B.S. degree in electrical engineering from Tsinghua University, China, in 2002. He is currently working toward the Ph.D. degree at the Department of Electrical and Computer Engineering, Center for Optical Technologies, Lehigh University, Bethlehem, PA.

His current research interests include spectroscopy of chemical species from near infrared to THz region.

Yujie J. Ding (M'04–SM'06) received the B.S. degree from Jilin University, Changchun, China, in 1984, the M.S.E.E. degree from Purdue University, West Lafayette, IN, in 1987, and the Ph.D. degree from the Johns Hopkins University, Baltimore, MD, in 1990.

From 1990 to 1992, he was a Postdoctoral Fellow at the Johns Hopkins University, where later on he became an Associate Research Scientist. From 1992 to 1999, he was an Assistant and then an Associate Professor of physics at Bowling Green State University. From 1999 to 2002, he was an Associate Professor of physics at the University of Arkansas, Fayetteville. In 2002, he joined Lehigh University, Bethlehem, PA, where he is currently a Professor at the Department of Electrical and Computer Engineering, Center for Optical Technologies. He is the author or coauthor of more than published 135 refereed journal articles in optoelectronics, nonlinear optics, and quantum electronics. His current research interests include THz, far-infrared and mid-infrared generation, amplification, and detection, nanostructures and nanodevices, photovoltaic effect, and their applications.

Prof. Ding is a Fellow of Optical Society of America. He was the recipient of Class of 1961 Professorship from Lehigh University in 2003 and Outstanding Young Scholar Award from Bowling Green State University in 1996.

Ioulia B. Zotova received the B.S. degree from the Russian Mendeleev University of Chemical Technology, Moscow, Russia, in 1997, the M.S. degree from Bowling Green State University, Bowling Green, OH, in 1999, and the Ph.D. degree from the University of Arkansas, Fayetteville, in 2002.

Since 2003, she has been with ArkLight, Center Valley, PA. Her current research interests include THz devices and spectrometers and identifications and detections of biological and chemical agents.